g = molar Gibbs energy
P = pressure
R = gas constant
T = absolute temperature
v = liquid molar volume
x = liquid mole fraction
y = vapor mole fraction

Greek Letters

γ = activity coefficient
δ defined as $2B_{12} - B_{11} - B_{22}$
Λ_{12}, Λ_{21} = Wilson parameters
λ = Wilson energy parameter

Subscripts

i = component i
ij = interaction of i and j
1 = component 1
2 = component 2

Superscripts

E = excess
sat = saturated

LITERATURE CITED

1. Barker, J. A., *Australian J. Chem.*, 6, 207 (1953).
2. Cines, M. R., J. T. Roach, R. J. Hogan, and C. H. Roland, *Chem. Eng. Progr. Symposium Ser. No. 6*, **49**, 1 (1953).
3. Din, F., ed., "The Thermodynamic Functions of Gases," Butterworths, London (1956).
4. Eckert, C. A., and J. M. Prausnitz, *A.I.Ch.E. J.*, **11**, 886 (1965).
5. Lewis, G. N., M. Randall, K. S. Pitzer, and L. Brewer, "Thermodynamics," 2 ed., Appendix 1, McGraw-Hill, New York (1961).
6. Mathot, V., *Nuovo Cimento*, **9**, Suppl. 1, 356 (1958).
7. Mathot, V., L. A. K. Staveley, J. A. Young, and N. G. Parsonage, *Trans. Faraday Soc.*, **52**, 1488 (1956).
8. Orye, R. V., and J. M. Prausnitz, *Ind. Eng. Chem.*, **57**, 18 (1965).
9. Pool, R. A. H., G. Saville, T. M. Herrington, B. D. C. Shields, and L. A. K. Staveley, *Trans. Faraday Soc.*, **58**, 1692 (1962).
10. Prausnitz, J. M., *Chem. Eng. Sci.*, **6**, 112 (1957).
11. Redlich, O., A. T. Kister, and C. E. Turnquist, *Chem. Eng. Progr. Symposium Ser. No. 2*, **48**, 49 (1952).
12. Sprow, F. B., and J. M. Prausnitz, *Trans. Faraday Soc.*, **62**, 1097 (1966).
13. Van Ness, H. C., "Classical Thermodynamics of Non-Electolyte Solutions," Macmillan, New York (1964).
14. Wilson, G. M., *J. Am. Chem. Soc.*, **86**, 127 (1964).

Manuscript received October 4, 1965; revision received February 11, 1966; paper accepted February 14, 1966.

A Fundamental Analysis of Slurry Grinding

H. E. TURNER and H. E. McCARTHY

E. I. du Pont de Nemours and Company, Wilmington, Delaware

An analytical approach to mathematical expression of the mechanisms involved in typical slurry grinders is presented. Experimental equipment performance is correlated with developed formulas. Results are expressed in terms of fundamental machine and slurry parameters useful in predicting performance and scale-up.

Wet grinding methods are frequently preferred over dry grinding where economic and product considerations permit, because wet grinding generally produces finer particle sized products. In fine dry pulverizing or deagglomerating size ranges, surface forces come into action causing agglomeration or cushioning, with less efficient use of energy. This ultimately limits the particle fineness that can be obtained. The much higher viscosity of the liquid system reduces the mobility of the contained solids and markedly increases the effect of shear forces produced by equipment components, thereby increasing size reduction effects. Another factor which may favor wet grinding is the lowering by the liquid phase of the surface tension (surface free energy) of the solids. This reduces the stress required for fracture (*1*).

As the need for fine grinding increases to supply the demand for fine particle products, reactants, and the like, it is important to obtain a more fundamental definition of the mechanisms involved in wet or slurry grinding. Considerable attention has been given to particle or material grindability, with less to the definition of the grinding mechanisms involved in important types of fine wet grinders and homogenizers available commercially. Comparisons of equipment capabilities in relation to product requirements have largely been empirical and qualitative. Correlations of equipment capabilities have mostly been confined to such relationships as throughput capacity in tons per hour ground to a given fineness, or surface area, per horsepower-hour of energy consumed. Little quantitative fundamental information is available on machine capabilities in relation to specific product fineness variations. The choice of equipment, its design, and operation therefore tend to rest on empirical considerations with specific testing needed to determine results of milling changes.

Analytical approaches are available whose early applications give promise of guiding more surely the selection of kind of equipment and of refining its design or operation to meet specific product requirements better. The criterion of merit proposed for assessing mill capabilities is the calculated shear force generated in consequence of the liquid viscosity of the dispersed mixture and the local velocity gradient prevailing in the active grinding zone of the mill. It is this viscous shear force which disintegrates the solid particulate. Forces controlling agglomeration are probably predominately due to molecular attraction and act over very short distances less than 1 micron (*7*). These forces fall off rapidly as separation distances are increased. Solids cleavage force is therefore the important consideration, rather than total work, which is force times distance. Product particle size should therefore correlate accurately with the magnitude of shear force, which should lend itself to calculation.

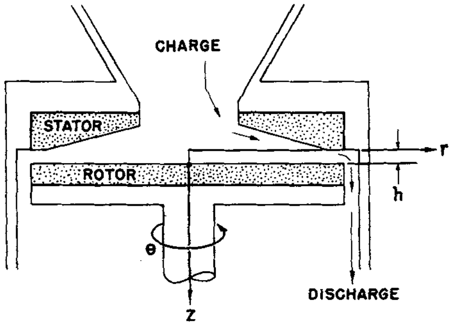

Fig. 1. Schematic representation of colloid mill showing axes.

Three representative slurry grinders or milling devices have been chosen to illustrate the analytical approach which should be applicable to almost any type of fine grinding: the colloid mill, rod mill, and high-speed mill (such as Kady) shown in Figures 1 to 3. Ball milling has been excluded from this class of grinding since impact crushing between the balls dominates.

The analytical approach to mathematical formula definition basically follows the methods of *Transport Phenomena* (2). Velocity gradients in space (or shear rate) are calculated from the equations of conservation of mass and momentum (simplified to meet the conditions and configurations of the various types of mills under consideration). Results are expressed as differentials in pertinent machine directions as dv/dh, where v is the local fluid velocity and h is the clearance between grinding surfaces.

Shear force is obtained by multiplying the vector shear rate by viscosity. Shear force developed under various milling conditions as calculated from these formulas is then compared with milling results to show correlation and verification of the approach. Formulas can then be utilized to predict required changes in milling conditions or designs to produce other results or for scale-up from small bench-scale equipment to large mills.

Temperature effect of shear has been neglected because estimation indicates only a rise of not over 10°C. and it is also a direct function of shear rate and viscosity (see Appendix).

It should be noted that efficiency of various types of grinding is also a factor in mill selection, since the means of effectively producing a given shear force is also important. This factor, however, is outside the scope of the present paper.

The development of formulas is outlined in the Appendix and results are summarized below.

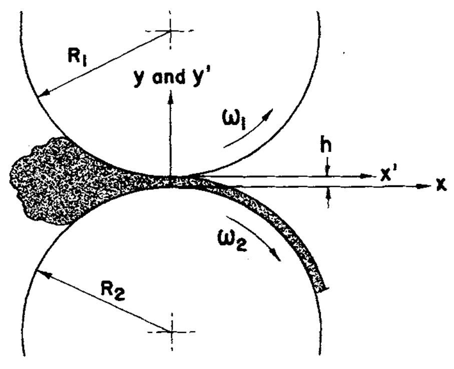

Fig. 2. Nip in bank of roll mill showing sets of axes.

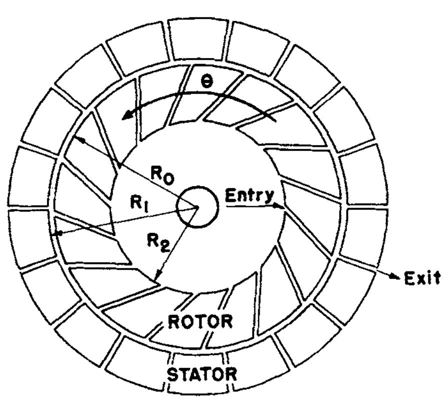

Fig. 3. Schematic representation of head of high-speed mill.

MATHEMATICAL MODELS OF SHEAR ACTION IN MILLS

Colloid Mill (Figure 1)

The shear rate at any point in the mill at radius r [see Equation (A-13) development] is given by

$$\dot{\gamma} = \frac{dv_\theta}{dz} = \frac{\alpha \omega r}{e^{\alpha h} - e^{-\alpha h}} (e^{\alpha z} + e^{-\alpha z}) \qquad (1)$$

where

$$\alpha = \sqrt{\frac{1}{r^2} + A} \qquad (2)$$

and

$$A = \frac{Q}{2\pi\, r\, h\nu} \qquad (3)$$

Note that the equation for shear rate can be expressed solely in terms representing mill dimensions or slurry properties.

Roll Mill (Figure 2)

The shear rate between any pair of rolls or radii r_1 and r_2 and clearance h [see development of Equation (A-38)] is given by

$$\dot{\gamma} = \frac{dv_x}{dy} = 6\left[\frac{\omega_1 r_1 + \omega_2 r_2}{2h_o^2} - \frac{Q}{h_o^3}\right](2y - h_o) + \frac{\omega_1 r_1 - \omega_2 r_2}{h} \qquad (4)$$

High-Speed Mill (Figure 3)

The shear rate at any point r [see Equation (A-22) development] is

$$\dot{\gamma} = \frac{dv_\theta}{dr} = \frac{\omega R_o^2}{R_o^2 - R_1^2}\left(1 - \frac{R_1^2}{r^2}\right) \qquad (5)$$

CORRELATION OF DATA WITH MODELS

Colloid Mill

Table 1 and Figure 4 summarize the results of calculating maximum shear rate at $z = h$ from Equations (1) to (3) for a series of seven runs in which a wax emulsion (coded A) was ground in a 4-in. diameter colloid mill with substantial variation in rotational speeds, stator-rotor clearances, and production rates at constant viscosity. Shear rate only (rather than shear force) is considered for simplicity, since viscosity is constant. Correlation is good and the curve tends to become asymptotic as zero particle size is approached. We would expect this asymptotic behavior since forces which cause agglomeration are generally considered to be molecular attraction. These forces are proportional to the radius of the particle (7).

TABLE 1. CALCULATED COLLOID MILL SHEAR RATE VS. WAX EMULSION A PARTICLE SIZE DETERMINED EXPERIMENTALLY

Mill speed, rev./min.	Mill clearance, in.	Production rate, gal./hr.	r = shear rate at $z = h$, sec.$^{-1}$	Average particle size, microns*
7,706	0.015	360	1.04×10^5	6.5
7,706	0.010	200	1.63×10^5	5.25
7,706	0.007	140	2.33×10^5	3.25
7,706	0.004	70	4.04×10^5	2.75
7,706	0.003	60	5.00×10^5	2.5
12,900	0.010	200	2.67×10^5	4.0
12,900	0.005	120	5.30×10^5	2.25

* By microscopic examination.
Note: Mill radius = 2 in.; slurry viscosity = 5.2 centipoise at 27% solids concentration.

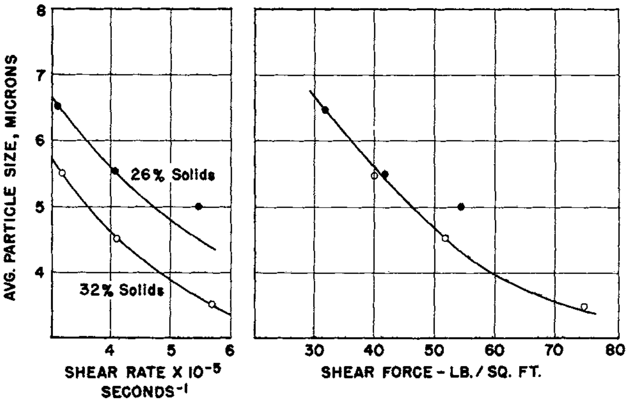

Fig. 5. (*Left*) Shear rate vs. particle size. (*Right*) Shear force vs. particle size.

The separating forces are proportional to the square of the radius. We could then predict that the shear force should be proportional to the radius to minus one power. The actual data show shear stress proportional to the radius to the minus three-halves power.

Table 2 and Figure 5 summarize the effect of viscosity and show that the shear force calculated by the developed formula accounts for viscosity well, since the two separate curves for shear rate condense into one smooth curve when a correction is made for the viscosities of the two different solids concentrations involved. The discrepancy in the high shear point at 25% solids concentration is considered to be experimental error.

Applicability of the approach to another material is shown in Figure 6 and Table 3 where wax emulsion *B* results are given. It should be particularly noted that with essentially identical shear rates, shear stress varies widely with the change in viscosity; the resulting variation in particle size is as predicted from the postulated approach.

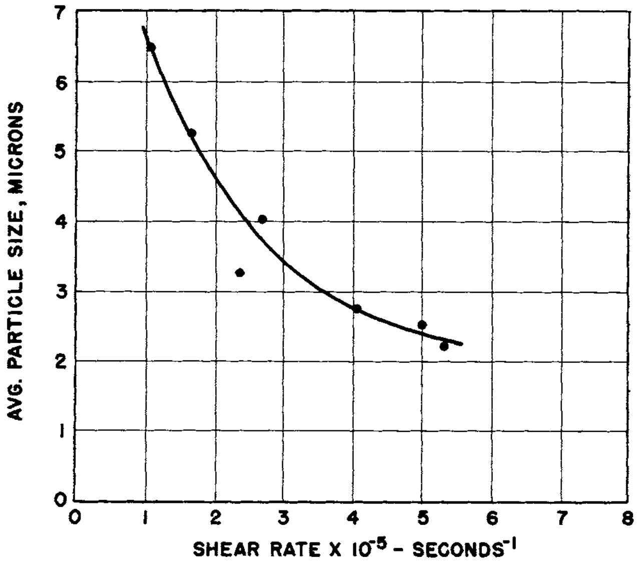

Fig. 4. Correlation of colloid mill shear rate vs. particle size produced.

Roll Mill and High-Speed Mill

Table 4* and Figure 7 present data and calculated

* Tabular material has been deposited as document 8872 with the American Documentation Institute, Photoduplication Service, Library of Congress, Washington, D. C., and may be obtained for $1.25 for photoprints or 35-mm. microfilm.

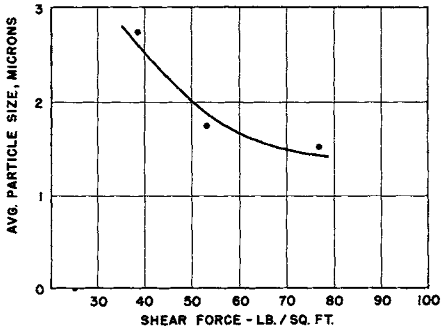

Fig. 6. Particle size vs. calculated shear force at various viscosities.

TABLE 2. CALCULATED COLLOID MILL SHEAR FORCE WITH VARYING VISCOSITY VS. WAX EMULSION A PARTICLE SIZE DETERMINED EXPERIMENTALLY

Mill speed, rev./min.	Mill clearance, in.	Production rate, gal./hr.	r = shear rate at $z = 0$,* sec.$^{-1}$	Viscosity,† (lb.)(sec.)/sq. ft.	τ = shear force $= \mu r$, lb./sq. ft.	Average particle size, microns
7,706	0.005	100	3.16×10^5	1.27×10^{-4}	40.2	5.5
7,706	0.004	70	4.08×10^5	1.27×10^{-4}	51.9	4.5
7,706	0.003	60	5.68×10^5	1.27×10^{-4}	74.8	3.5
7,706	0.005	240	3.04×10^5	1.03×10^{-4}	31.3	6.5
7,706	0.004	180	4.02×10^5	1.03×10^{-4}	41.4	5.5
7,706	0.003	120	5.26×10^5	1.03×10^{-4}	54.2	5.0

* Chosen for simplification since calculations in Table 1 showed an average error of 1% incurred by using $z = 0$ instead of $z = h$.
† Viscosity was calculated by Thomas' extension of Einstein's analysis (6) based on 32 and 26% solids concentration, respectively, for the first three and the last three runs. Liquid viscosity was 2 centipoise.

Table 3. Variation in Particle Size and Calculated Shear Force at Various Fluid Viscosities but Identical Shear Rates

Mill speed, rev./min.	Mill clearance, in.	Production rate, gal./hr.	r = shear rate at $z = 0$,* sec.$^{-1}$	Viscosity,† (lb.)(sec.)/sq. ft.	τ = shear force = μr, lb./sq. ft.	Average particle size, microns
12,900	0.003	32	8.86×10^5	2.14×10^{-4}	3.84×10^2	2.75
12,900	0.003	30	9.00×10^5	3.04×10^{-4}	5.31×10^2	1.75
12,900	0.003	20	9.04×10^5	4.10×10^{-4}	7.70×10^2	1.50

* Chosen for simplification since calculations in Table 1 showed average error of 1% incurred by using $z = 0$ instead of $z = h$.
† Viscosity was calculated by Thomas' extension of Einstein's analysis (6) based on 21, 30, and 40% solids concentration, respectively. Liquid viscosity was 2 centipoise.

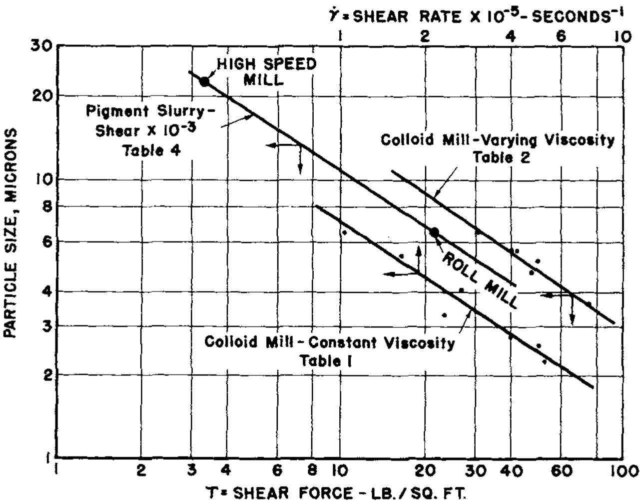

Fig. 7. Performance comparison of roll mill, high-speed mill, and colloid mill.

shear force for experimental milling of a pigment slurry in a five-roll mill and a high-speed mill (*middle line*). While only two points were determined, they correlate very well with other data on the log-log plot. The two experimental runs were with different viscosities, again indicating that viscosity has been adequately taken into consideration in the formulas. The small divergence of slopes (0.66, 0.67, and 0.69) indicates an overall high degree of correlation and suggests that average particle size of material produced in slurry grinders varies inversely with the two-thirds power of the shear force; or conversely, the shear force required for grinding varies inversely with the 1.5 power of particle diameter (accepted grinding theory ascribes a range of 1 to 2 for the particle diameter exponent). Thus, the analytical approach has the advantage over empirical approaches not only in providing an insight into relationships of individual variables to shear rate and shear stress, but also has provided a relationship between shear force and resultant particle size. The approach and relationships developed should be useful in analyzing performance and/or design of slurry grinding mills.

ACKNOWLEDGMENT

Appreciation is expressed for review of the work and comments by Dr. J. H. Olson of the University of Delaware. The comments on temperature effect of shear and the colloid mill analysis were of particular assistance.

Figures 1 and 3 are reproduced by permission of Morehouse-Cowles, Inc., and by Kinetic Dispersion Corporation, respectively.

NOTATION

a = cross-sectional area, sq.ft.
h = clearance between mill components in grinding zone, ft.
P = pressure, lb./sq.ft.
Q = quantity flow rate, cu.ft./sec.
r = radius, ft.
T = temperature, °C.
U = velocity, ft./sec.
v = velocity, ft./sec.
$\mathbf{v}$ = mass average velocity, ft./sec.
z = coordinate direction, ft.

Greek Letters

$\dot{\gamma}$ = shear rate, sec.$^{-1}$
θ = coordinate direction
μ = viscosity of the liquid, (lb.)(sec.)/sq.ft.
ν = kinematic viscosity of the liquid, sq.ft./sec.
ρ = density of the liquid, lb./cu.ft.
τ = shear force, liquid, lb./sq.ft.
ω = angular velocity, rad./sec.
Φ_v = viscous dissipation function, sec.$^{-2}$
ϕ = time, sec.

Subscripts

r = in radial direction
z = in z direction
x = in x direction
y = in y direction
θ = in tangential direction

Superscript

$\wedge$ = per unit mass

Mathematical Operations

D/Dt = substantial derivative
∇ = del or nabla operator

LITERATURE CITED

1. Adamson, A. W., "Physical Chemistry of Surfaces," p. 235, Interscience, New York (1960).
2. Bird, R. B., E. N. Lightfoot, and W. E. Stewart, "Transport Phenomena," pp. 80, 85, Wiley, New York (1960).
3. *Ibid.*, p. 83.
4. Patton, T. C., "Paint Flow and Pigments Dispersion," p. 345, Interscience, New York (1964).
5. Schlichting, Hermann, "Boundary Layer Theory," pp. 98-104, McGraw-Hill, New York (1960).
6. Thomas, D. G., *Ind. Eng. Chem.*, **55**, 21 (1963).
7. Dzyaloshinski, I. E., E. M. Lifshitz, and L. P. Pitaevskii, *Advan. Phys.*, **10**, 165 (1961).

APPENDIX

Development of the formulas listed in the body of the text is outlined below. The approach will be illustrated first by its application to a typical colloid mill (see Figure 1). By applying the methods of "*Transport Phenomena*" (2), the Navier-Stokes equation (for Newtonian fluids) can be derived from the equation of motion and expressed in cylindrical coordinates in terms of velocity gradients. Since there is no flow in the z direction and symmetry exists with respect to the axis of rotation, the expressions simplify to

r component:

$$\rho\left(v_r\frac{\partial v_r}{\partial r}-\frac{v_\theta^2}{r}\right)=\mu\left[\frac{\partial}{\partial r}\left(\frac{1}{r}\frac{\partial}{\partial r}(rv_r)\right)+\frac{\partial^2 v_r}{\partial z^2}\right]+\frac{dP}{dr} \quad \text{(A-1)}$$

ϵ component:

$$\rho\left(v_r\frac{\partial v_\theta}{\partial r}+\frac{v_r v_\theta}{r}\right)=\mu\left[\frac{\partial}{\partial r}\left(\frac{1}{r}\frac{\partial}{\partial r}(r v_\theta)\right)+\frac{\partial^2 v_\theta}{\partial z^2}\right] \quad \text{(A-2)}$$

These equations are valid for laminar or viscous flow which occurs in the extremely thin films (0.001 to 0.005 in.) present in the type of equipment under consideration.

If we assume that no fluid slippage occurs at the fluid solid interfaces of rotor and stator, then at $z = h$

$$v_\theta = \omega r$$

and

$$\partial v_\theta/\partial r = \omega = \text{constant}$$

at

$$z = 0$$

$$v_\theta = 0$$

To simplify the Navier-Stokes equation, the following equation of continuity is developed for the system (3):

$$\frac{1}{r}\frac{\partial}{\partial r}(r\,v_r)+\frac{1}{r}\frac{\partial}{\partial\theta}v_\theta=0 \quad \text{(A-3)}$$

since v_θ does not vary with θ

$$\partial(r\,v_r)/\partial r=0 \quad \text{(A-4)}$$

and this term drops out of Equation (A-1).

To simplify further, since the nip or clearance is small in the r direction

$$\text{average } v_r=\frac{Q}{a}=\frac{Q}{2\pi rh}\text{ where } h = \text{clearance} \quad \text{(A-5)}$$

$$\text{let } A=\frac{v_r}{\nu}=\frac{Q}{2\pi h\nu} \quad \text{(A-6)}$$

and the equation in the θ component becomes

$$\frac{\partial^2 v_\theta}{\partial r^2}+\frac{\partial^2 v_\theta}{\partial z^2}+\left(\frac{1}{r}-A\right)\frac{\partial v_\theta}{\partial r}-\left(\frac{1}{r^2}+\frac{A}{r}\right)v_\theta=0 \quad \text{(A-7)}$$

By taking r as a constant which is valid for analysis of differential shear at any given radius, it follows that

$$\frac{d^2 v_\theta}{dz^2}-\left(\frac{1}{r^2}+\frac{A}{r}\right)v_\theta=0 \quad \text{(A-8)}$$

By rearranging and dividing by v_θ

$$\frac{1}{v_\theta}\frac{d^2 v_\theta}{dz^2}=\left(\frac{1}{r^2}+\frac{A}{r}\right) \quad \text{(A-9)}$$

the solution to which is

$$v_\theta=\left(-e^{-z\sqrt{\frac{1}{r^2}+\frac{A}{r}}}+e^{z\sqrt{\frac{1}{r^2}+\frac{A}{r}}}\right)B \quad \text{(A-10)}$$

where B is an arbitrary constant.

For boundary conditions

$$\text{At } z=h \qquad v_\theta=\omega r$$

$$\text{At } z=0 \qquad v_\theta=0$$

In solving for B, let

$$\alpha=\sqrt{\frac{1}{r^2}+A}$$

At $z = h$

$$B(-e^{-\alpha h}+e^{\alpha h})=\omega r$$

and

$$B=\frac{\omega r}{e^{\alpha h}-e^{-\alpha h}} \quad \text{(A-11)}$$

and Equation (A-10) becomes

$$v_\theta=\frac{\omega r}{e^{\alpha h}-e^{-\alpha h}}\left(e^{z\sqrt{\frac{1}{r^2}+\frac{A}{r}}}-e^{-z\sqrt{\frac{1}{r^2}+\frac{A}{r}}}\right) \quad \text{(A-12)}$$

The shear rate at any point in the mill is

$$\frac{dv_\theta}{dz}=\frac{\alpha\omega r}{e^{\alpha h}-e^{-\alpha h}}(e^{\alpha z}+e^{-\alpha z}) \quad \text{(A-13)}$$

As previously, the shear rate can be calculated directly for any point in the grinding zone.

The High-Speed Mill

The high-speed mill (Figure 3) grinds by differential shearing velocity in the close clearance between an internal rotating circular member and an external stationary member. This force actually predominates over impact, as will be developed later. The mathematical analysis procedure is similar to that of the colloid mill. The Navier-Stokes equation under steady state conditions and for $v_r = v_z = 0$ becomes

r component:

$$-\frac{v_\theta}{r}=-\nu\frac{2}{r^2}\frac{\partial v_\theta}{\partial\theta}-\frac{1}{\rho}\frac{dP}{dr} \quad \text{(A-14)}$$

θ component:

$$\frac{v_\theta}{r}\frac{\partial v_\theta}{\partial\theta}=\nu\left[\frac{\partial}{\partial r}\left(\frac{1}{r}\frac{\partial}{\partial r}(r\,v_\theta)\right)+\frac{1}{r^2}\frac{\partial^2 v_\theta}{\partial\theta^2}\right] \quad \text{(A-15)}$$

The equation of continuity is

$$\frac{1}{r}\frac{\partial}{\partial\theta}(rv_\theta)=0 \quad \text{(A-16)}$$

since $(\partial v_\theta/\partial\theta) = 0$, the second term of Equation (A-14), as well as the terms involving $(dv_\theta/d\theta)$ of Equation (A-15), drops out and the equations reduce as follows:

$$\frac{d^2 v_\theta}{dr^2}+\frac{1}{r}\frac{dv_\theta}{dr}-\frac{v_\theta}{r^2}=0 \quad \text{(A-17)}$$

solving

$$v_\theta=C_1 r+\frac{C_2}{r} \quad \text{(A-18)}$$

Boundary conditions at

$$r=R_o \text{ then } v_\theta=\omega R_o$$

and at

$$r=R_1 \text{ then } v_\theta=0$$

Solving

$$C_2=-C_1R_1^2 \quad \text{(A-19)}$$

$$C_1=\frac{\omega R_o^2}{R_o^2-R_1^2} \quad \text{(A-20)}$$

then

$$v_\theta=\frac{\omega R_o^2}{R_o^2-R_1^2}\left(r-\frac{R_1^2}{r}\right) \quad \text{(A-21)}$$

where

$$R_o\leq r\leq R_1$$

The shear rate at any point in the Kady mill is

$$\dot{\gamma} = \frac{dv_\theta}{dr} = \frac{\omega R_o^2}{R_o^2 - R_1^2}\left(1 - \frac{R_1^2}{r^2}\right) \qquad (A\text{-}22)$$

To use this equation as the total shear rate, it must be shown that the impact force can be disregarded in a particular mill. Experimental work reported herein was done in a (laboratory) Model L Kady Mill. Typical shear rates are 1×10^5 sec.$^{-1}$. An upper limit on impact velocities would be of the order of 10 to 20 ft./sec. By considering the high shear rate existent and the relatively large amount of surface available for shear (64% of circumference since slots are ⅛ in. wide), it is concluded that the dominant effect is that of shear.

Roll Mill

Shear mechanisms prevalent in the roll mill include not only those caused by differential machine velocities, but also pressure gradients caused by the compressive force from narrowing of the roll nip on the viscous media.

Expressing the equation of motion (2) in rectangular coordinates, one obtains

$$\rho\, v_x \frac{\partial v_x}{\partial x} + \frac{\partial P}{\partial x} = \mu\left(\frac{\partial^2 v_x}{\partial x^2} + \frac{\partial^2 v_x}{\partial y^2}\right) \qquad (A\text{-}23)$$

(The second term, the pressure differential, did not exist in the analyses of previous mills. Note that $v_z = 0$, and that y component is neglected since v_y is very small.)

The change in v_x with x is small compared to the change with respect to y, so (A-23) reduces to

$$\rho\, v_x \frac{\partial v_x}{\partial x} + \frac{dP}{dx} = \mu \frac{\partial^2 v_x}{\partial y^2} \qquad (A\text{-}24)$$

To analyze the pressure term, take the equation of continuity in the form

$$\text{per unit of length, } Q = \int_o^{h(x)} U\,dy = \text{constant} \qquad (A\text{-}25)$$

If we take the equation of motion for viscous parallel flow with an imposed pressure gradient (5)

$$\frac{dP}{dx} = \mu \frac{\partial^2 v_x}{\partial y^2} \qquad (A\text{-}26)$$

At boundary conditions

$$\text{at } y = 0 \quad v_x = U_2(x, y) = U_2 \quad \text{at } x = 0 \quad P = P_o$$

$$y = h \quad v_x = U_1(x, y) = U_1 \qquad x = x_\infty \quad P = P_o$$

Integrating and rearranging Equation (A-26) one obtains

$$\frac{\partial v_x}{\partial y} = \frac{1}{\mu}\frac{dP}{dx} y + C_1 \qquad (A\text{-}27)$$

By integrating

$$v_x = \frac{1}{2\mu}\frac{dP}{dx} y^2 + C_1 y + C_2 \qquad (A\text{-}28)$$

at $y = 0$

$$C_2 = U_2$$

at $y = h$

$$U_1 = \frac{1}{2\mu}\left(\frac{dP}{dx}\right) h^2 + C_1 h + U_2 \qquad (A\text{-}29)$$

By substituting for C_1 and C_2, Equation (A-28) becomes

$$v_x = \frac{1}{2\mu}\frac{dP}{dx}(y^2 - hy) + U_1 \frac{y}{h} + U_2\left(1 - \frac{y}{h}\right) \qquad (A\text{-}30)$$

In order to use Equation (A-30), it must be shown that $\rho\, v_x(\partial v_x/\partial x)$ is small and can be neglected [since from Equation (A-23) it is a part of the total indicated shear mechanism]. To consider this aspect, analyze (dU/dx) where U = average velocity in the nip of the rolls. For the specific case of two 4-in. diameters of the rolls in rectangular coordinates

$$h = h_o + 2y' \qquad (A\text{-}31)$$

y' expressed in rectangular coordinates is

$$y' = 2 - \sqrt{4 - x^2} \qquad (A\text{-}32)$$

The following equations are developed:

$$\frac{dh}{dx} = \frac{4x}{(4 - x^2)^{1/2}} \qquad (A\text{-}33)$$

$$\frac{dU_x}{dx} = -\frac{Q}{h^2}\frac{dh}{dx} \qquad (A\text{-}34)$$

Arithmetic computation shows that near the nip the velocity shear term is on the order of 0.06 lb./sq.in., whereas the pressure shear term is on the order of 10^3 to 10^4 lb./sq.in., justifying the simplification.

By translating Equation (A-30) into usable form, for a unit length

$$Q = aU = hU = \int_o^h \left\{ \frac{1}{2\mu}\frac{dP}{dx}(y^2 - hy) + U_1 \frac{y}{h} + U_2\left(1 - \frac{y}{h}\right)\right\} dy \qquad (A\text{-}35)$$

By solving

$$\frac{dP}{dx} = 12\mu\left[\frac{U_1 + U_2}{2h^2} - \frac{Q}{h^3}\right] \qquad (A\text{-}36)$$

Restating Equation (A-30), one obtains

$$v_x = \frac{1}{2\mu}\frac{dP}{dx}(y^2 - hy) + U_1 \frac{y}{h} + U_2\left(1 - \frac{y}{h}\right) \qquad (A\text{-}37)$$

By substituting (A-36) into (A-30) and by differentiating, at the nip ($U_1 = \omega_1 r_1$ and $U_2 = \omega_2 r_2$)

$$\dot{\gamma} = \frac{dv_x}{dy} = 6\left[\frac{\omega_1 r_1 + \omega_2 r_2}{2h_o^2} - \frac{Q}{h_o^3}\right](2y - h_o) + \frac{\omega_1 r_1 - \omega_2 r_2}{h} \qquad (A\text{-}38)$$

Clearly the first term on the right-hand side, the pressure term, dominates the shear rate, as the differential velocity between the rolls will be the smaller term.

Temperature Effect of Shear

An analysis of the temperature effect of shear is necessary to determine its significance. From Bird, Lightfoot, and Stewart, the general equation of energy (10.1-20) is

$$\rho \hat{C}_v \frac{DT}{Dt} = k\nabla^2 T - T\left(\frac{\partial p}{\partial T}\right)_P (\nabla \cdot \mathrm{v}) + \mu\Phi_v \qquad (A\text{-}39)$$

The term of interest is the heat input due to viscous dissipation or the dissipation function $\mu\Phi_v$. For unidirectional flow in a shear plane

$$\mu\Phi_v = \mu\left(\frac{dv_x}{dy}\right)^2 = \mu(\dot{\gamma})^2 \qquad (A\text{-}40)$$

First consider shear in the roll mill, since it has both highest shear rate and viscosity. Analysis will be carried out in c.g.s. units for convenience.

$$\mu = 50 \text{ poises}$$

$$\dot{\gamma} = 2 \times 10^5 \text{ sec.}^{-1}$$

By taking $C_p = 1$ and $\rho = 2$; ϕ = residence time (3.64×10^{-5} sec.)

$$\Delta T = \frac{\mu(\dot{\gamma})^2 \phi}{\rho C_p} = 0.88°\text{C.}$$

Thus the temperature effect of shear is negligible and would be so except in cases of very high viscosity. A similar analysis was made for the Kady mill, since it has a longer residence time. Temperature rise in this case was also negligible.

Manuscript received September 20, 1965; revision received February 10, 1966; paper accepted February 10, 1966. Paper presented at A.I.Ch.E. Philadelphia meeting.